We are IntechOpen,
the world's leading publisher of
Open Access books
Built by scientists, for scientists

6,900
Open access books available

186,000
International authors and editors

200M
Downloads

Our authors are among the

154
Countries delivered to

TOP 1%
most cited scientists

12.2%
Contributors from top 500 universities

CLARIVATE ANALYTICS
BOOK CITATION INDEX
INDEXED

WEB OF SCIENCE™

Selection of our books indexed in the Book Citation Index
in Web of Science™ Core Collection (BKCI)

Interested in publishing with us?
Contact book.department@intechopen.com

Classification of Mental Tasks using Different Spectral Estimation Methods

Pablo F. Diez[1], Eric Laciar[1], Vicente Mut[2], Enrique Avila[1], Abel Torres[3]
[1] Gabinete de Tecnología Médica, Universidad Nacional de San Juan
[2] Instituto de Automática, Universidad Nacional de San Juan
[3] Departament ESAII, Universitat Politècnica de Catalunya
[1,2]Argentina, [3]Spain

1. Introduction

The electroencephalogram (EEG) is the non-invasive recording of the neuronal electrical activity. The analysis of EEG signals has become, over the last 20 years, a broad field of research, including many areas such as brain diseases (Parkinson, Alzheimer, etc.), sleep disorders, anaesthesia monitoring and more recently, in new augmentatives ways of communication, such as Brain-Computer Interfaces (BCI).

BCI are devices that provide the brain with a new, non-muscular communication channel (Wolpaw *et al.*, 2002), which can be useful for persons with motor impairments. A wide variety of methods to extract features from the EEG signals can be used; these include spectral estimation techniques, wavelet transform, time-frequency representations, and others. At this moment, the spectral estimation techniques are the most used methods in the BCI field.

The processing of EEG signals is an important part in the design of a BCI (Wolpaw *et al.*, 2002). It is commonly divided in the features extraction and the feature translation (Mason & Birch, 2003). In this work, we will focus in the EEG features extraction using three different spectral estimation techniques.

In many studies, the researchers use different spectral estimation techniques like Fourier Transform (Krusienski *et al.*, 2007), Welch periodogram (Millán *et al.*, 2002); (Millán *et al.*, 2004) or Autoregressive (AR) modeling (Bufalari *et al.*, 2006); (Krusienski *et al.*, 2006); (Schlögl *et al.*, 1997) in EEG signals. A review of methods for features extraction and features translation from these signals can be found in a review from the Third BCI meeting (McFarland *et al.*, 2006). A comparison between the periodogram and the AR model applied to EEG signals aimed to clinical areas is presented in (Akin & Kiymik, 2000). Finally, an extended comparison of classification algorithms can be found in (Lotte *et al.*, 2007).

In this chapter, we compare the performance of three different spectral estimation techniques for the classification of different mental tasks over two EEG databases. These techniques are the standard periodogram, the Welch periodogram (both based on Fourier transform) and Burg method (for AR model-based spectral analysis). For each one of these methods we compute two parameters: the mean power and the root mean square (RMS) in

different frequency bands. Both databases used in this work, are composed by a set of EEG signals acquired on healthy people. One database is related with motor-imagery tasks and the other one is related with math and imagery tasks.

The classification of the mental tasks was conducted with different classifiers, such as, linear discriminate analysis, learning vector quantization, neural networks and support vector machine.

This chapter is organized as follows. In the next section the databases utilized in this work are explained. The section 3 contains a description of the estimation spectral methods used. An explanation of the procedure applies to each database is arrived in section 4. The different classifiers are briefly described in section 5 and the obtained results are shown in section 6. Finally, in sections 7 and 8 a discussion about results and the conclusions are presented.

2. EEG Databases

In this work, we have used two different databases, each one with diverse mental tasks.

2.1. Math-Imagine database

This database was collected in a previous work (Diez & Pi Marti, 2006) in the Laboratory of Digital Electronics, Faculty of Engineering, National University of San Juan (Argentina). EEG signals from the scalp of six healthy subjects (4 males and 2 females, 28±2 years) were acquired while they performed three different mental tasks, namely: *(a) Relax task:* the subjects close his eyes and try to relax and think in nothing in particular; *(b) Math Task:* the subjects make a regressive count from 3 to 3 beginning in 30, i.e. 30, 27, 24,...3, 0. The subjects were asked to begin the count once again and try to not verbalize; and *(c) Imagine task:* the subjects have to imagine an incandescent lamp at the moment that it is turn on.

For each subject, the EEG signals were acquired using six electrodes of Ag/AgCL in positions F_3, F_4, C_3, C_4, P_3 and P_4 according to the 10-20 positioning system. With this electrodes were configured 4 bipolar channels of measurement (ch1: F_3-C_3; ch2:F_4-C_4; ch3:P_3-C_3; ch4: P_4-C_4). Each channel is composed by an instrumentation amplifier with gain 7000 and CMRR greater than 90dB, a bandpass analogical filter set at 0.1-45Hz and an analogical to digital converter ADC121S101 of 12 bits accuracy with a sampling rate of 150Hz.
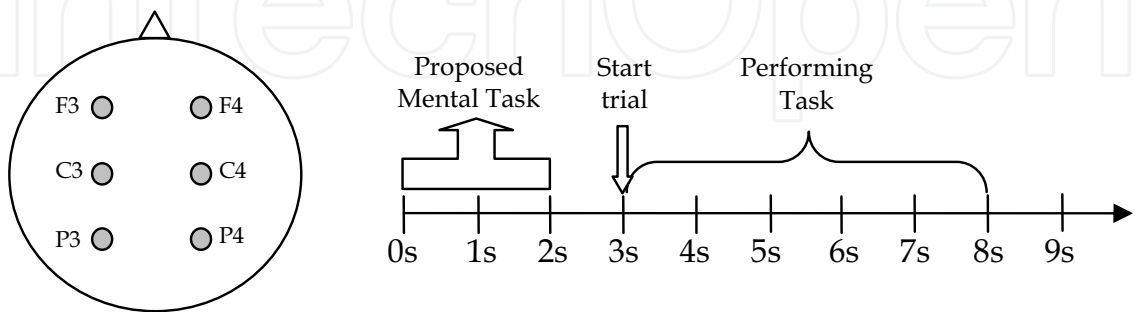

Fig. 1. Electrodes position indicated by grey circles (left), on F_3, F_4, C_3, C_4, P_3 and P_4 according to 10-20 positioning system. The acquisition protocol is presented on the right.

The subjects were trained to keep the maximal concentration while perform the mental tasks. Each mental task has a duration of 5s (750 samples) with 3s between them. The subjects were seated comfortably, with dim lighting, in front of a PC monitor. In which, were presented to subjects the proposed mental tasks (0-2s), the start signal to begin the trial (3s) and the final of the trial (8s), in according with the protocol illustrated in Figure 1. No feedback was presented to subjects during the trials. Every session had 15 trials for each mental task, i.e., 45 trials in total. Two subjects (Subj#1 and Subj#2) performed 3 sessions; the others performed only 2 sessions, i.e., two subjects had 135 trials and the rest 90 trials. The EEG of this database were digitally filtered using a Butterworth bi-directional bandpass filter, order 10, with 6 and 40Hz as lower and upper cut-off frequencies respectively.

2.2. Motor-Imagery database

This database was acquired in the Department of Medical Informatics, Institute for Biomedical Engineering, University of Technology Graz (Austria) and it is available free on-line from http://ida.first.fraunhofer.de/projects/bci/competition_iii/ (BCI-Competition III web page). It was recorded from a normal subject (female, 25 years) during a feedback session. The subject sat in a relaxing chair with armrests. The task was to control a feedback bar by means of *(a) imagery left hand* and *(b) imagery right hand* movements. The order of left and right cues was random. The experiment consists of 140 trials, conducted on the same day.

Each trial had the first 2s in silence, at t=2s an acoustic stimulus indicates the beginning of the trial and a "+" was displayed for 1s; then at t=3s, an arrow (left or right) was displayed as cue. At the same time the subject was asked to move a bar into the direction of the arrow (Figure 2). Similar acquisition protocols were implemented in several studies (Schlögl *et al.*, 1997); (Neuper *et al.*, 1999). The recording was made using a G.tec amplifier and Ag/AgCl electrodes. Three bipolar EEG channels (anterior '+', posterior '-') were measured over C_3, C_z and C_4. The EEG was sampled with 128 Hz and analogically filtered between 0.5 and 30 Hz. The feedback was based on AAR parameters of channel over C_3 and C_4, the AAR parameters were combined with a discriminate analysis into one output parameter.

Each EEG record of the motor-imagery database was digitally filtered using a Butterworth filter, order 8, with 6 and 30 Hz as lower and upper cut-off frequencies respectively.
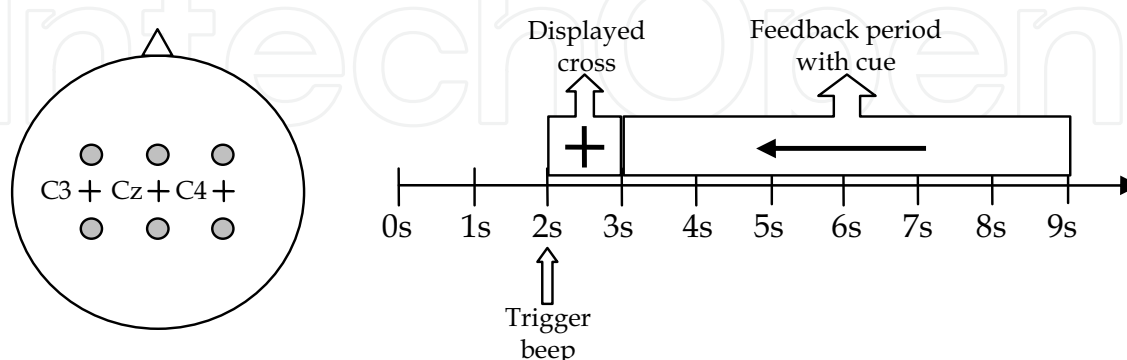

Fig. 2. Electrodes position indicated by grey circles (left), located ±2.5 cm over the crosses. The crosses indicates the position of C_3, C_Z and C_4 according to 10-20 positioning system. The acquisition protocol is presented on the right.

3. Spectral Analysis

EEG signals were processed in order to estimate the signal Power Spectral Density (PSD), this section explain the different PSD estimation methods regardless the database used. The three analysed techniques were: (a) standard periodogram, (b) Welch periodogram and (c) Burg method.

3.1. Standard Periodogram

The periodogram is considered as a non-parametric spectral analysis since no parametric assumptions about the signal are incorporated.

This technique was introduced at an early stage in the processing of EEG signals and it is based in the Fourier Transform. Considering that EEG rhythms are essentially oscillatory signals, its decomposition in terms of sine and cosine, was found useful (Sörnmo & Laguna, 2005). Basically, the Fourier spectral analysis correlates the signal with sines and cosines of diverse frequencies and produces a set of coefficients that defines the spectral content of the analyzed signal. The Fourier Transform computed in the discrete field is known as Discrete Time Fourier Transform (DTFT).

Thus, the periodogram is an estimation of the PSD based on DTFT of the signal $x[n]$ and it is defined by the following equation:

$$\hat{S}_P(f) = \frac{T_s}{N} \left| \sum_{n=1}^{N} x[n] e^{-j2\pi f n T_s} \right|^2 \tag{1}$$

where $S_P(f)$ is the periodogram, T_S is the sampling period, N is the number of samples of the signal and f is the frequency. Hence, the periodogram is estimated as the squared magnitude of the N points DTFT of $x[n]$. The DTFT is easily computed through the Fast Fourier Transform (FFT) algorithm and, therefore, also the periodogram.

A variation of the periodogram is the windowed periodogram, i.e., we apply a window, in the process of computing periodogram. Each kind of window has specific characteristics. There are many types of windows, such as triangular windows (like Bartlett's), gaussian windows (like Hanning's) and others kinds. These windows are used to deal with the problem of smearing and leakage, due to the presence of main lobe and side lobes. For more details see (Sörnmo & Laguna, 2005).

In the standard periodogram, no window is used (although no using window is the same as using a rectangular window).

In Figure 3, it is presented two periodograms (computed with a 1024 points FFT) of EEG signals from Motor-Imagery database, where an Event Related Desynchronization (ERD) is observed (Pfurtscheller & Lopes da Silva, 1999). That means, in channel 1 over C_3 (left figure) the mean power in μ-band (8 to 12 Hz) is higher than the other one in channel 2 over C_4 (right figure), i.e., in this trial, it is observed easily that subject imagines a left motor task.
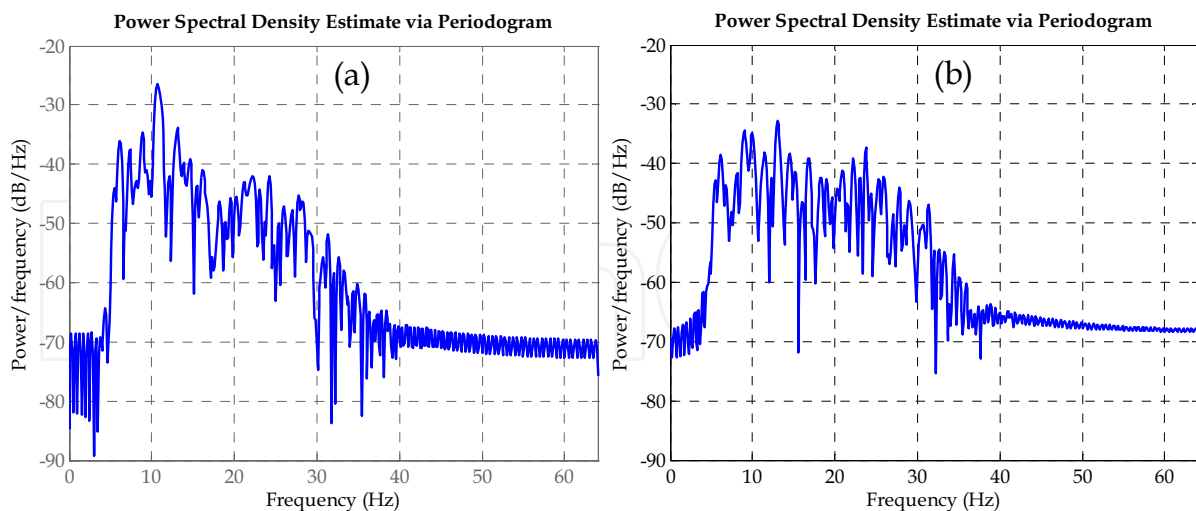
Fig. 3. Standard Periodograms from Motor-Imagery database, trial n°1, between 4 to 6 s; from (a) channel 1 (over C$_3$) and (b) from channel 2 (over C$_4$). In this trial the subject imagines a left motor task, then the mean power in μ-band over C$_4$ is lower than C$_3$. Both periodograms were estimated with a 1024 points FFT. EEG signals were previously filtered between 6 and 30 Hz.

3.2. Welch Periodogram

Welch periodogram is a version modified of the periodogram, it can use windowing or not, but the principal feature of this method is the averaging periodogram. The consequence of this averaging is the reduction of the variance of the spectrum, at the expense of a reduction of spectral resolution

The Welch periodogram can be computed performing the following steps:

1. Split the signal in M overlapped segments of D samples length each.
2. Calculates the periodogram for each segment $S_P(f)^{(m)}$. Each segment had applied a window.
3. Hence, the Welch periodogram $S_W(f)$ is calculated as:

$$\hat{S}_W(f) = \frac{1}{M} \sum_{m=1}^{M} \hat{S}_P(f)^{(m)} \tag{2}$$

The quantity of segments M could be calculated as:

$$M = \frac{N-D}{L} + 1 \tag{3}$$

where N is the number of samples of the signal and L is the number of samples overlapping between the segments. In this work, the overlapping was selected in 50% in all cases, which is the standard value in computation of Welch periodogram.

The resolution R depends on the length of segment D according to:

$$R = \frac{1}{DT_S} \tag{4}$$

Hence, high values of D (higher than 75 %, approximately, of the number of samples of the signal N) obtain a PSD similar to the standard periodogram. On the contrary, with small values of D the periodogram is smoothed. This fact can be observed in the Figure 4, where several Welch periodogram are shown, for different Hamming window lengths (16, 32, 64 and 128 points).
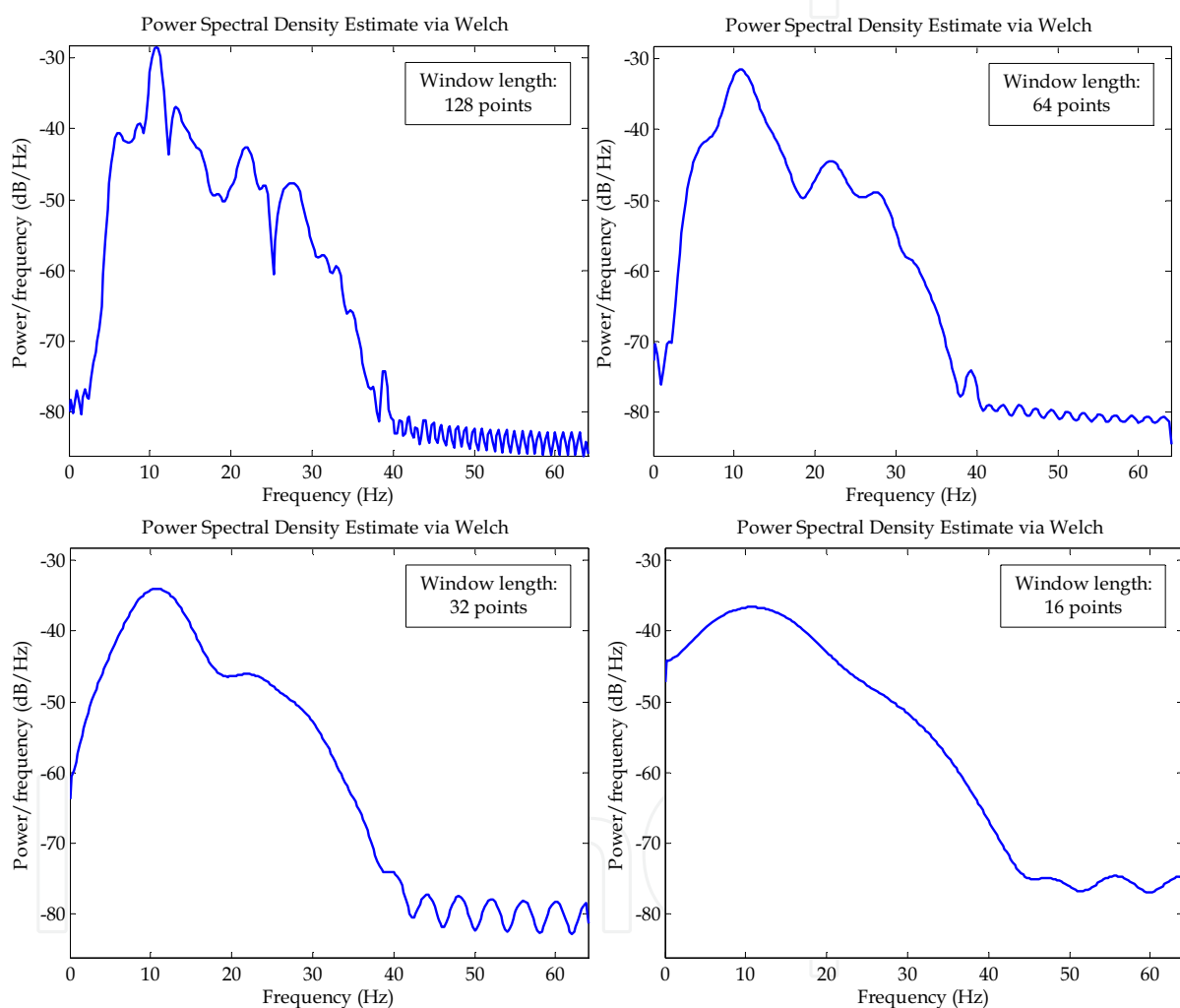

Fig. 4. Welch periodogram computed with a 512 points FFT, for different window length (128, 64, 32 and 16 points), from Motor-Imagery database, trial nº1, between 4 to 6 s; from channel 1 (over C$_3$). The periodogram is smoothed when decreasing the window length. A Hamming window was applied in all cases. The EEG signal was filtered between 6 to 30 Hz.

3.3. Burg method

If consider the EEG like a linear stochastic signal, the EEG can be modelled as an autoregressive (AR) model, i.e., the estimation of PSD becomes a problem of system identification.

An AR modelling is, as depicted in Figure 5, based on white noise $v_{(n)}$ feeding a filter $H_{(z)}$, thus we obtain the signal $x_{(n)}$. The white noise is considered as zero-mean and variance σ_v^2. The filter $H_{(z)}$ is expressed as:

$$H_{(z)} = \frac{1}{A_{(z)}} = \frac{1}{1 + a_1 z^{-1} + a_2 z^{-2} + \cdots + a_p z^{-p}} \tag{5}$$

where $A_{(z)}$ is a polynomial of order p with coefficients a_p. Those can be estimated through different methods, such as autocorrelation (Yule-Walker), covariance, modified covariance and Burg method. In this work, the Burg method was utilized.

Once we are estimated the coefficients a_p, the PSD is calculated as:

$$S(f) = \frac{T_s \sigma^2}{\left| 1 + \sum_{p=1}^{P} a_p \, e^{-j2\pi f T_s p} \right|^2} \tag{6}$$

where σ is the variance of the input signal and P is the order of the AR model.

The Burg method is a technique to estimate the coefficients a_p of the AR model. This method joint the minimization of the forward and backward prediction error variances using the Levinson-Durbin recursion in the minimization process. The prediction error filter is estimated using a lattice structure; afterwards, the parameters are transformed into direct form FIR predictor parameters. Thus, the PSD can be calculated using (6). The Burg description algorithm is beyond of the scope of this work, for mathematical concerns see (Sörnmo & Laguna, 2005).
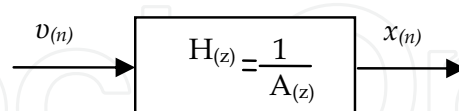

Fig. 5. Autoregressive modeling: Modeled signal $x_{(n)}$ obtained through filtering white noise $v_{(n)}$ with filter $H_{(z)}$.

3.3.1. Model order

An issue in parametric PSD is choosing the model order, since it influences the shape of estimated PSD. A low order means a smooth spectrum and, on the other hand, a high order results in a PSD with spurious peaks. One more pair of roots of polynomial $A_{(z)}$, i.e., increase the model order in two, force another peak in the estimated spectrum.

There are a few criteria to estimate "the best order" of the model. These criteria penalises the complexity of the model when increasing the model order. The most known criteria are the

Final Prediction Error (FPE), Akaike and modified Akaike (minimum description length of Rissanen).

For a signal of length N, the penalty function of each criterion is:

$$FPE_{(p)} = \frac{N+p}{N-p}\sigma_e^2 \tag{7}$$

$$AIC_{(p)} = N \ln \sigma_e^2 + 2p \tag{8}$$

$$AIC_{Modif(p)} = N \ln \sigma_e^2 + p \ln N \tag{9}$$

where σ_e^2 is the prediction error variance.

Figure 6 illustrates the penalty function of the different criteria and it is indicated the best order found for each method. It was observed, generally, that Akaike and FPE methods provide the same order of AR model, whereas the modified Akaike criterion does not. Besides, Akaike and FPE usually overvalue the order of AR model, therefore, it would be preferable to use the modified Akaike criterion.

In this work, the three criteria were tested, unfortunately, no reliable results were found. This is, the optimal order varies for each method, also varies for every acquisition channel, and for data of the same mental task. Hence, the Burg method was analyzed for several orders on each database, regardless of the order determined by the mentioned criteria.
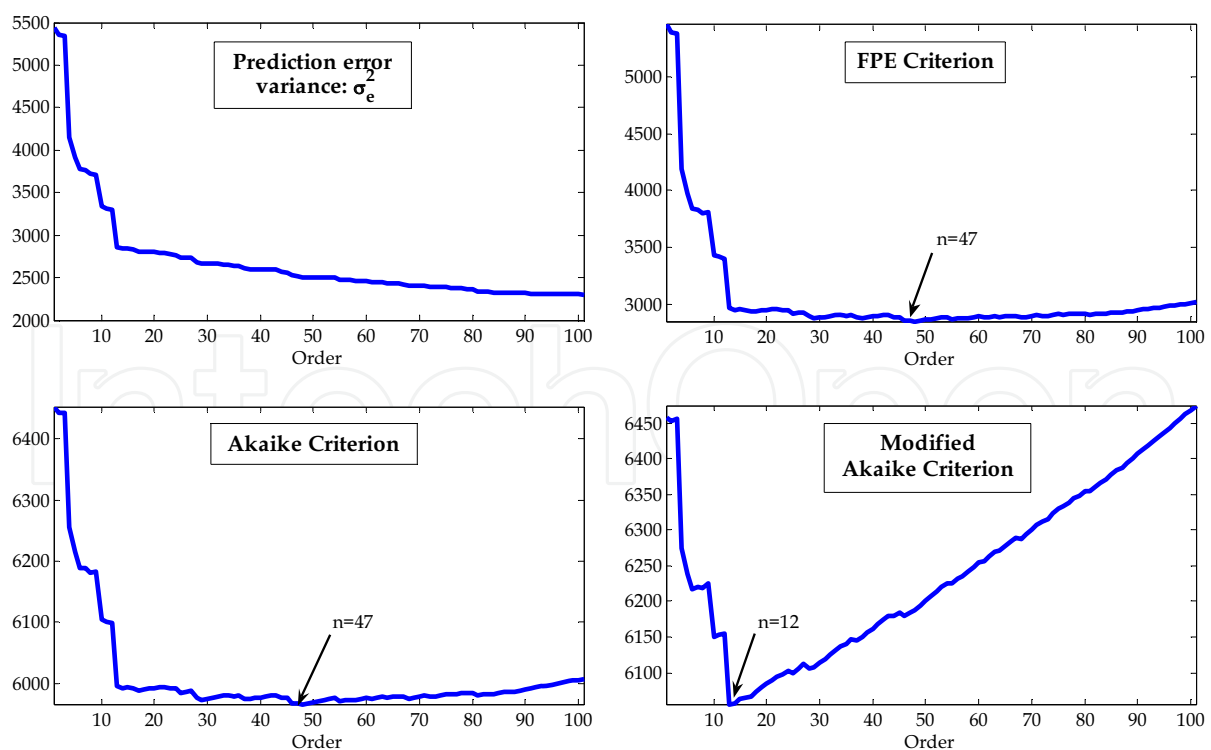

Fig. 6. Penalty functions of the different criteria (σ_e^2, FPE, Akaike and Modified Akaike), analyzed on Math-Imagery database, channel 2 in first trial.
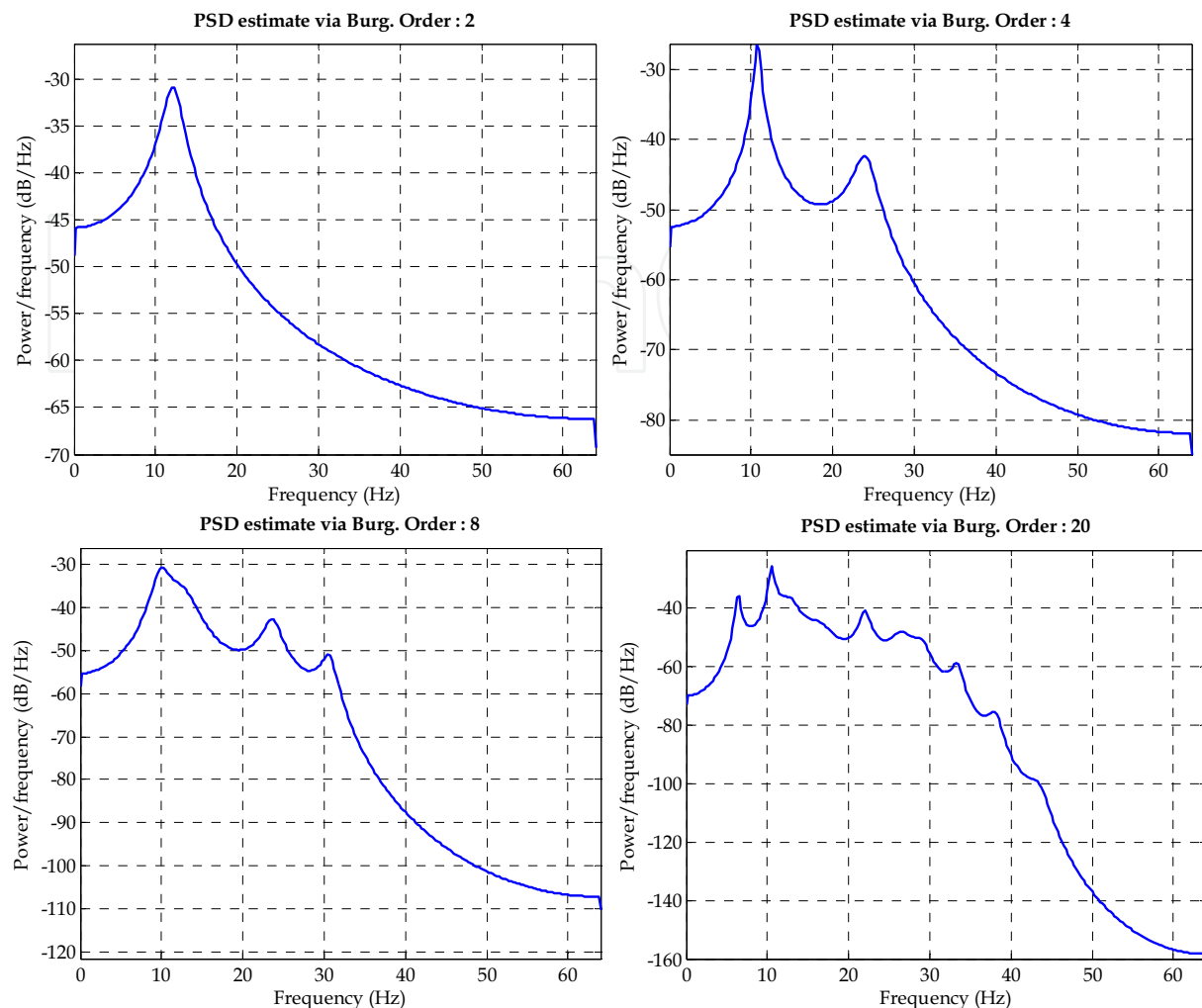
Fig. 7. PSD estimated under Burg method for different order of AR model (2, 4 8 and 20). The spectrum has more peaks when increase the order, according to *nº of peaks= AR model order/*2.

4. Features Extraction

Although, the three proposed PSD estimation methods were apply on both databases, special concerns need to be considered for each database. In this section, it is presented an explanation on the way that each PSD method was applied on each database.

4.1. Features extraction on Math-Imagery database

As was explained in section 2, the signals of this database were filtered between 6 and 40 Hz. The range of frequencies utilized includes the bands α (8 to12Hz), β (12 to 27 Hz), γ (> 27 Hz) and a part of θ-band (6 to 8Hz). The γ-band is utilized due to the improvement results shown in (Palaniappan, 2006).

For this database, we proposed a little different division of the EEG bands. The periodograms were split in bands and sub-bands according to Table I. Due to the shape of

the EEG spectrum (for higher frequencies, lower amplitudes), each sub-band is wider than precedent sub-band. This is with the intention of compensation on the values of parameters calculated.

The standard periodogram was calculated using a 1024 points FFT with zero padding, allowing a frequency resolution of 0.147 Hz. The Welch periodogram, for our 750 samples signal, was computed using a Hamming window of lengths *D=300, D=100* and *D=50*, with 50% overlapping. The Burg method was computed for various orders of the AR model, ranging from 5 to 50.

The PSD estimation methods were computed using the complete duration of trial after cue signal, i.e., a signal of 5 s.

Bands	Frequency (Hz)
Pre-α	6 to 8
α	8 to 12
β1	12 to 14
β2	14 to 18
β3	18 to 25
γ1	25 to 32
γ2	32 to 40

Table 1. Bands and sub-bands in which the PSD estimation methods were divided when applied on the Math-Imagery database. The pre-α band, is just the half of θ band.

4.2. Features extraction on Motor-Imagery database

This database was digitally filtered, as explained in section 2, between 6 and 30 Hz. In this case, the μ (8 to 12 Hz) and β (14 to 30 Hz) bands are on focus, since we tracking the Event Related Synchronization/Desyncronization (ERS/ERD) related with Motor-Imagery (Pfurtscheller & Lopes da Silva, 1999).

The subjects performed the mental task over a period of 6 s (see Figure 2), but the different PSD estimation were computed over a period of 2 s included between 4 s to 6 s. This is performed in this way due to the best results were found over this period of time (Ferreira *et al.*, 2008).

The standard periodogram was calculated using 1024 points FFT with zero padding, allowing a frequency resolution of 0.125 Hz.

For the computing of Welch periodogram were utilized Hamming windows of 128, 64, 32 and 16 points length, always with a 50% overlapping and with 512 points FFT.

The Burg method was computed using several orders of the AR model, between 4 up to 20 in steps of 2.

4.3. Spectral parameters

For the proposed bands in each database, two parameters were computed: the mean Power (P_m) and the Root Mean Square (RMS) of the signal, both evaluated in frequency domain. They are calculated as:

$$P_m = \sum_{k=L}^{H} S(k) \qquad (10)$$

$$RMS = \sqrt{\sum_{k=L}^{H} S(k)} \qquad (11)$$

where $S(k)$ are the sampled values of the periodogram $S(f)$, L and H are the indexes corresponding to the higher and lower sampled frequency values for each analyzed sub-band.

4.4. Feature Vector

The feature vector is the input vector presented to the classifier. There were two configuration of the input vector:

- Using the P_m of the frequency bands.
- Using the RMS of the frequency bands.

These configurations were used with the three estimation methods of the PSD.

5. Classification

The classification was conducted with some different classifier for each database in order to the results were unbiased by the classifier.

For the Math-Imagery database the classifiers used were: a Linear Discriminate Analysis (LDA), a Learning Vector Quantization (LVQ). This classification was performed for the three mental tasks at the same time. To validate the results the Leave-One-Out Cross-Validation method was utilized.

For the motor-imagery dataset were implemented a LDA, a Multilayer Perceptron (MLP) and a Support Vector Machine (SVM).

For a comparison of most used classifiers algorithms in BCI see (Lotte *et al.*, 2007). Following a briefly description of each method used in this work:

5.1. Linear Discriminate Analysis

Basically, the LDA is a linear combination of variables, on the form:

$$y_{km} = u_0 + u_1 X_{1km} + u_2 X_{2km} + \cdots + u_p X_{pkm} \qquad (12)$$

where y_{km} is the value of the discriminate function for the case m on the group k, X_{ikm} is the discriminate variable X_i for the case m on the group k, u_i are the required coefficients (with $i=1, 2, …, p$).

The number of discriminate functions is determined by the number of considered groups. Thus, the values of all discriminate functions (needed to separate all groups between them)

determine the belonging group of the considered case. For more detailed concerns see the specific bibliography (Tinsley & Brown, 2000);(Gil *et al.*, 2001).

5.2. Learning Vector Quantization

The LVQ is essentially a kind of neural network; it was based in the self-organizing map (Kohonen, 1990) as first layer and a second layer of linear perceptrons. The first layer is trained with a competitive algorithm with the concept of neighbouring. The linear layer transforms the competitive layer's classes into the target classifications. For more detailed explanation of LVQ see (Kohonen, 1990) and (Haykin, 1999).

The LVQ was used, only, to classify the mental tasks on Math-Imagery database. The architecture was 50 neurons on competitive layer and 3 neurons in second layer. This layer is the output layer and each neurons represents a different mental task, i.e., only one neuron can be active at time.

The LVQ was trained by 300 epochs, this value was determined in a preliminary experiment using a subset of the entire data. The same procedure was implemented to determine the number of neurons in the competitive layer.

5.3. Multilayer Perceptron

Possibly, this may be the more spread used neural network in general applications. The MLP was composed with an input layer, two hidden layers and an output layer. The input layer has the same size of the input feature vector, the output layer has many neurons as classes to classify and the neurons in hidden layers are determined empirically. In this case, 10 and 5 neurons are placed in the first and second hidden layer, respectively.

The training algorithm utilized was the Levenberg-Marquardt backpropagation with an early-stopping method (Haykin, 1999).

5.4. Support Vector Machine

SVM is another tool used BCI for the classification of EEG. The SVM maps input vectors into a higher dimensional space where the classification can be easily. Then SVM finds a linear separating hyperplane with the maximal margin in this higher dimensional space.

Given a training set of instance-label pairs *(x_i; y_i)*; i = 1, ..., l where $x_i \in \Re^n$ and $y \in \Re^l$ such that $y_i \in \{1, -1\}$, the SVM require the solution of the following optimization problem:

$$\min_{w,b,\xi} \quad \frac{1}{2} w^T w + C \sum_{i=1}^{l} \xi_i$$

$$\text{subject to} \quad y_i \left(w^T \phi(x_i) + b \right) \geq 1 - \xi_i \tag{13}$$

$$\xi_i \geq 0$$

where *C* is the penalty parameter of the error term ξ_i. The kernel function used in this work is a radial basis function on the form:

$$K(x_i, x_j) \equiv \phi(x_i)^T \phi(x_j) = e^{-\gamma \|x_i - x_j\|^2}, \gamma > 0 \qquad (14)$$

Therefore, for the implementation of a SVM is needed to determine the parameters C and γ. The searching of C and γ is conducted through a grid-search using cross-validation (Hsu *et al.*, 2008). The SVM used in this work is the one implemented in LIBSVM (Chang & Lin, 2008). Finally, it was implemented two cross-validation schemes nested, an inner loop cross-validation in order to determine the parameters C and γ and an outer cross-validation in order to evaluate the performance of the SVM.

6. Results

In this section we present the results obtained in this work. In the case of Math-Imagery database, the results were obtained using a Leave-one-out-cross-validation scheme and in the case of Motor-Imagery dataset, the presented results were attained using a 10-fold-cross-validation repeated over 10 times, i.e., a 10x10-fold-CV (this is performed in order to achieve a more accuracy results).

Figure 8 and 9 show the results obtained with the standard periodogram on Math-Imagery and motor-imagery databases, respectively. In Figure 8, the accuracy achieved by the LDA is better than LVQ (except in S2) and RMS feature allows obtaining better results. In Figure 9, the performances of classifiers are similar, but once again RMS presents better results than P_m.

The results obtained with Welch periodogram on Math-Imagery database are presented in Figure 10, forthe different chosen window length. The optimal window length varies for each subject. The difference between P_m and RMS is not so clear, but still remains a little superiority of RMS. In Figure 11, are presented the results on motor-imagery dataset, we can see a superiority of RMS over P_m. The performance of LDA and MLP are similar, but the SVM are a little inferior.
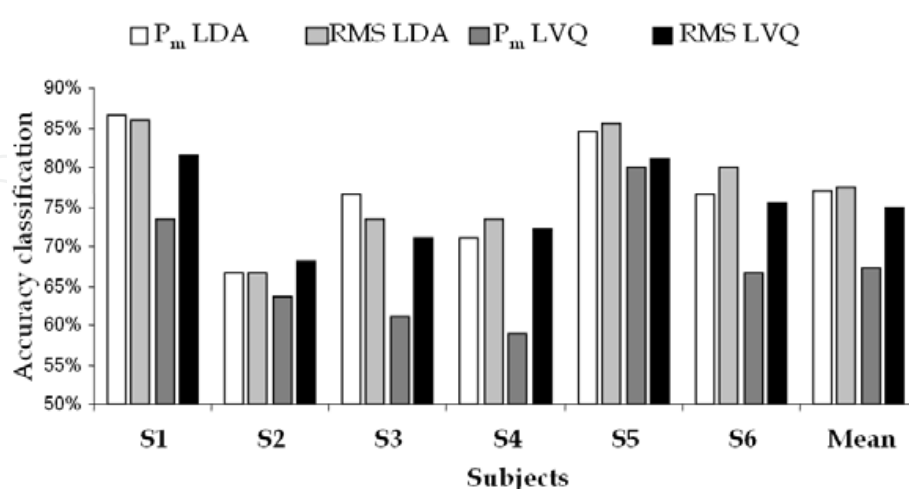

Fig. 8. Results attained with the standard periodogram, the bars represent the accuracy obtained using the Pm and RMD of bands with LDA and LVQ evaluated in the non-traditional database.
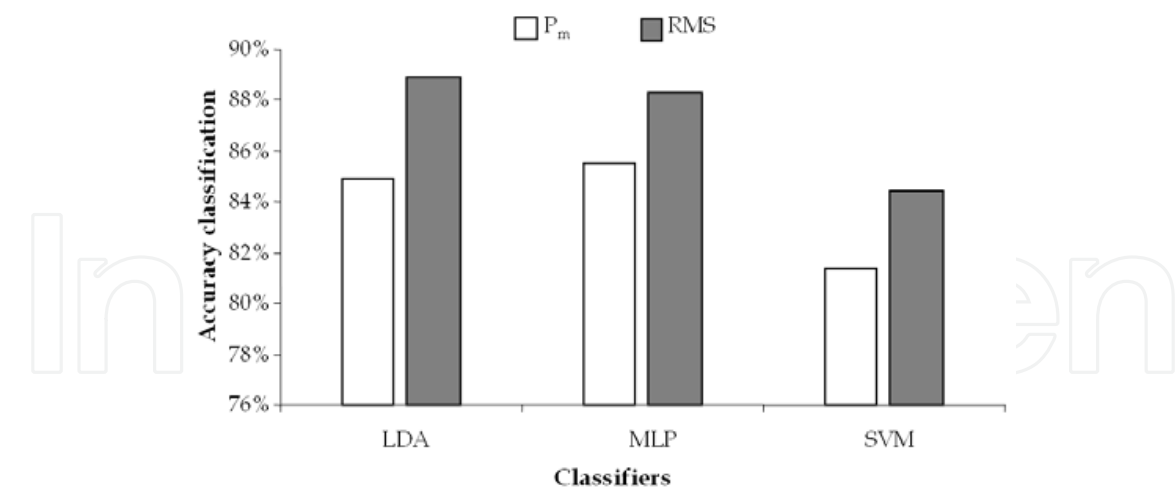
Fig. 9. Accuracy classification on motor-imagery dataset using standard periodogram for three proposed classifiers.
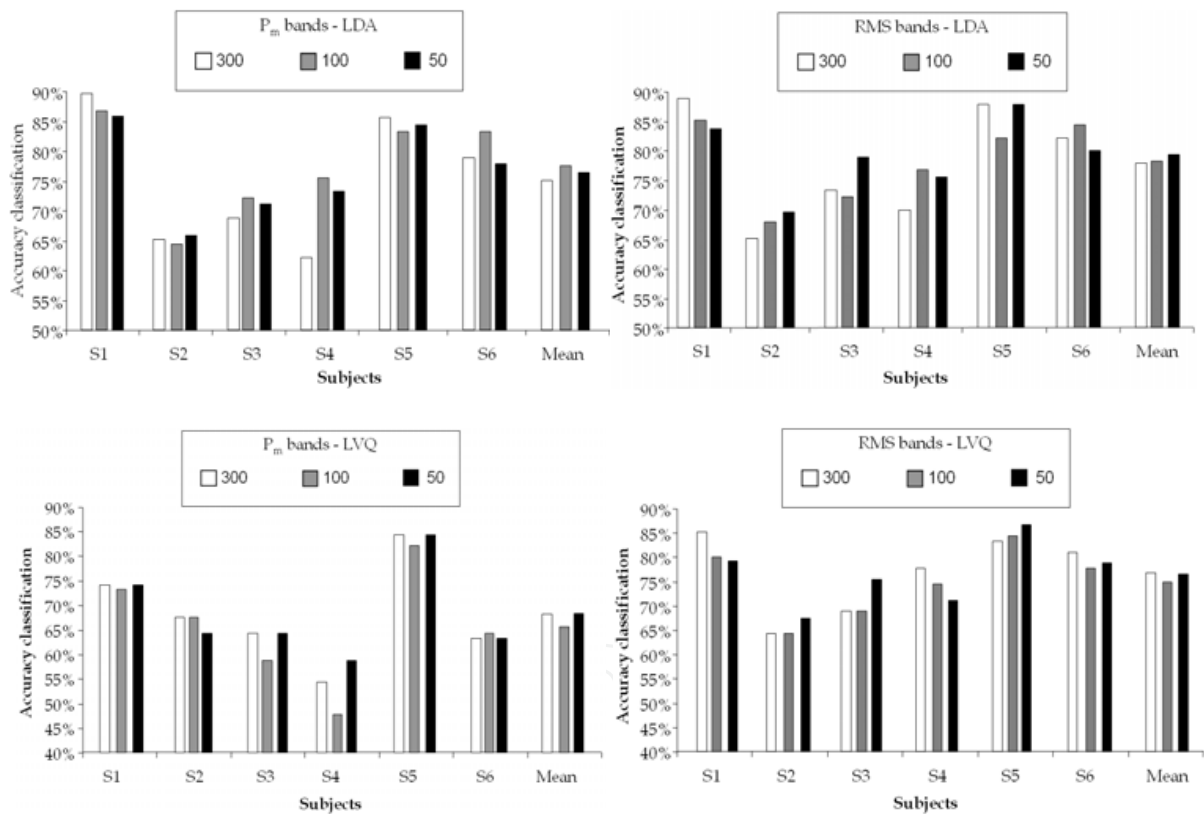

Fig. 10. Results obtained using LDA with Welch periodogram, for different window lengths. The length were 300, 100 and 50 all with 50% overlapping, for a signal of 750 samples duration

With Burg method, the results are presented in Figure 12 for the motor-imagery dataset and for the Math-Imagery database the values of accuracy classification are shown in Table 2 and Table 3. The order of AR model that allows the better accuracy classification is different for each subject, but generally the RMS performance is better than P_m.

Finally, a comparison of the best results attained with each PSD estimation method is presented in Figures 13 and 14. For the Math-Imagery dataset, it is observed in Figure 13 that the best results are obtained using Welch periodogram or Burg method. Similar results are obtained using LDA or using LVQ.

For the motor-imagery dataset, in Figure 14, it is shown the best results obtained for each classifier proposed for this dataset.
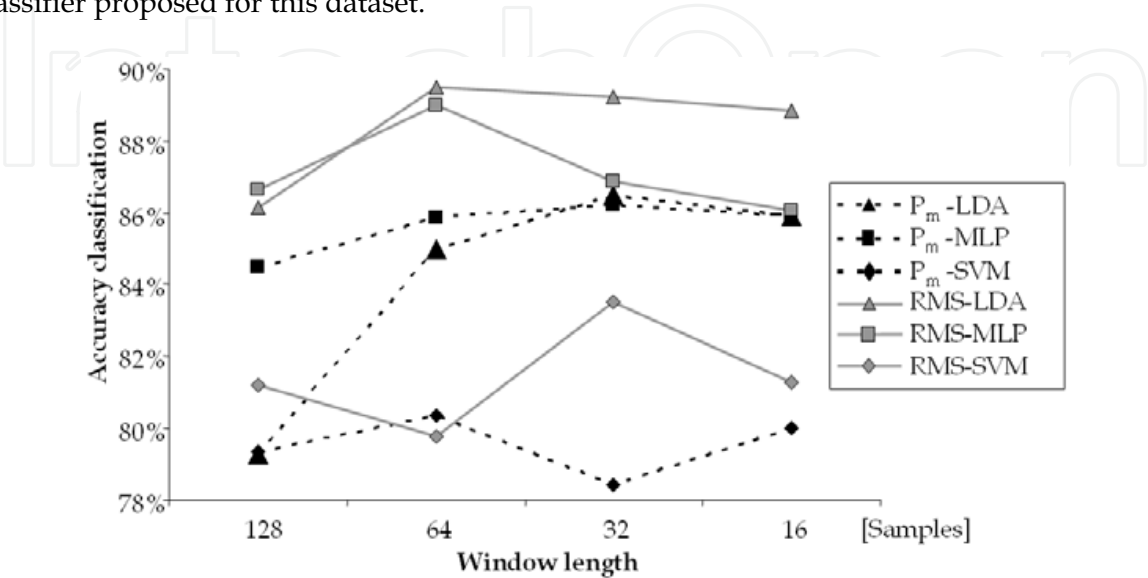

Fig. 11. Accuracy classification obtained with Welch periodogram for LDA (▲), MLP (■) and SVM (♦). The features are calculated using the Pm (dashed black line) and RMS features (continuous grey line).
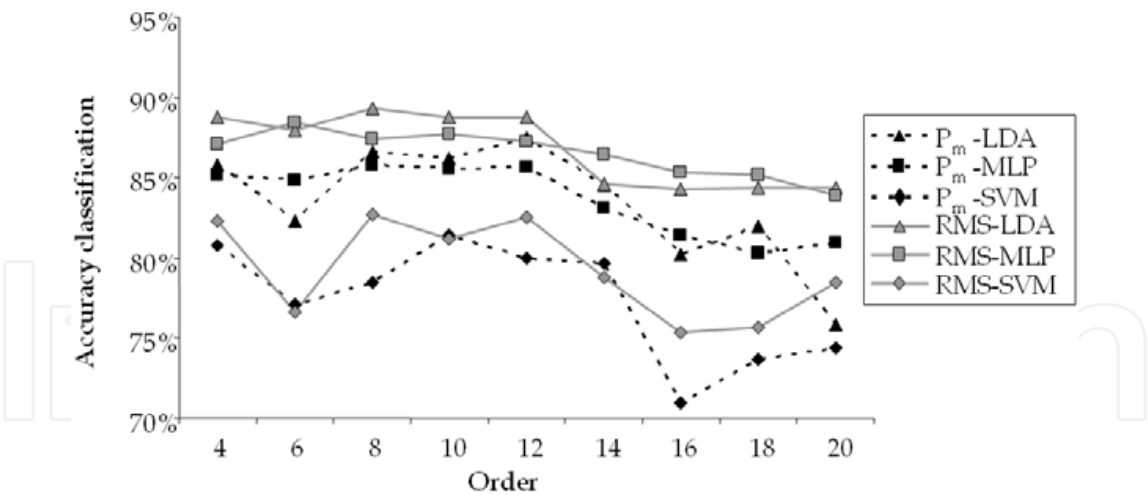

Fig. 12. Accuracy classification obtained with Burg method on motor-imagery dataset for different order of AR model with LDA (▲), MLP (■) and SVM (♦). The features are calculated using the mean power (dashed black line) and RMS (continuous grey line).
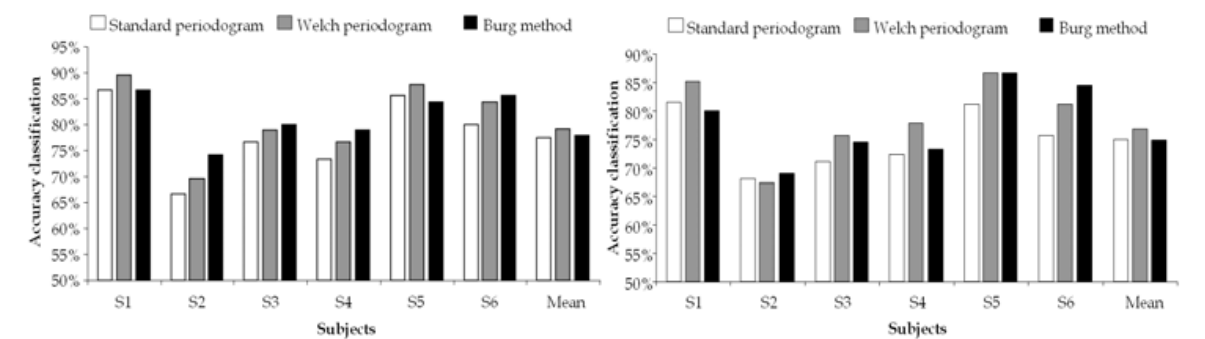
Fig. 13. Best accuracy classification obtained with each PSD estimation method proposed with the LDA (left) and LVQ (right) on Math-Imagery database.

	Order	S1	S2	S3	S4	S5	S6	Mean	Std.
P$_m$	5	80,0%	74,1%	80,0%	70,0%	78,9%	80,0%	**77,2%**	4,2%
	10	84,4%	67,4%	67,8%	68,9%	81,1%	77,8%	**74,6%**	7,5%
	15	82,2%	66,7%	72,2%	73,3%	80,0%	80,0%	**75,7%**	6,0%
	20	84,4%	64,4%	72,2%	75,6%	78,9%	77,8%	**75,6%**	6,8%
	30	85,2%	65,2%	71,1%	77,8%	75,6%	77,8%	**75,5%**	6,8%
	40	77,0%	61,5%	65,6%	71,1%	82,2%	78,9%	**72,7%**	8,1%
	50	81,5%	61,5%	68,9%	75,6%	76,7%	76,7%	**73,5%**	7,1%
RMS	5	80,0%	72,6%	75,6%	67,8%	81,1%	83,3%	**76,7%**	5,9%
	10	85,2%	63,0%	71,1%	73,3%	80,0%	83,3%	**76,0%**	8,4%
	15	85,2%	66,7%	74,4%	75,6%	80,0%	85,6%	**77,9%**	7,2%
	20	84,4%	63,7%	74,4%	78,9%	84,4%	82,2%	**78,0%**	8,0%
	30	84,4%	68,9%	73,3%	77,8%	80,0%	81,1%	**77,6%**	5,6%
	40	85,2%	69,6%	71,1%	74,4%	83,3%	81,1%	**77,5%**	6,6%
	50	86,7%	68,1%	70,0%	76,7%	82,2%	82,2%	**77,7%**	7,4%

Table 2. Accuracy classification obtained with Burg method and LDA on Math-Imagery database. The higher values for each subject are shaded.

	Orden	S1	S2	S3	S4	S5	S6	Media	Std.
P$_m$	5	68,2%	64,4%	67,8%	58,9%	80,0%	67,8%	**67,8%**	6,9%
	10	70,4%	65,9%	63,3%	50,0%	83,3%	66,7%	**66,6%**	10,7%
	15	73,3%	62,2%	58,9%	54,4%	82,2%	64,4%	**65,9%**	10,1%
	20	70,4%	62,2%	58,9%	48,9%	76,7%	65,6%	**63,8%**	9,6%
	30	72,6%	64,4%	58,9%	58,9%	80,0%	66,7%	**66,9%**	8,2%
	40	74,1%	66,7%	62,2%	60,0%	83,3%	61,1%	**67,9%**	9,15
	50	71,9%	61,5%	65,6%	50,0%	84,4%	64,4%	**66,3%**	11,4%
RMS	5	73,3%	66,7%	68,9%	72,2%	85,6%	76,7%	**73,9%**	6,6%
	10	80,0%	62,2%	74,4%	67,8%	86,7%	75,6%	**74,4%**	8,6%
	15	79,3%	62,9%	68,9%	68,9%	83,3%	77,8%	**73,5%**	7,7%
	20	77,1%	66,7%	66,7%	67,8%	86,7%	80,0%	**74,1%**	8,3%
	30	79,3%	65,2%	67,8%	72,2%	83,3%	75,6%	**73,9%**	6,8%
	40	78,5%	68,9%	66,7%	67,8%	82,2%	84,4%	**74,8%**	7,9%
	50	79,3%	64,4%	66,7%	73,3%	86,7%	77,8%	**74,7%**	8,3%

Table 3. Accuracy classification obtained with Burg method and LVQ on Math-Imagery database. The higher values for each subject are shaded.

7. Discussion

Although the standard periodogram is the simplest method and does not need to chose parameters for its implementation (except the points of FFT), generally, it not presents the best accuracy achieved in the classification on each database.

In the other hand, the Welch periodogram and Burg method obtain better results than standard periodogram, but these methods present the difficulty of having to choose some parameters for its implementation. The window length parameter in Welch method is more intuitive to choose, since it represents the smoothing in the periodogram, i.e. with smaller window length more smoothed periodogram. For Burg method, the chosen of order of AR model is more difficult, since it exists a relationship between AR model order and the number of PSD peaks (number of peaks=AR model/2), which a-priori are unknown. This fact can be observed in Figure 7.

In Math-Imagery database, the results for the Welch periodogram show that the best results were obtained using the RMS parameter, except for Subj#1. Also, it can observed that $D=100$ and $D=50$ are the best choice for the window's length. The mean values shows that RMS obtained with $D=100$ has the best classification (81.78%), but the RMS obtained with $D=50$ is just a little bit lower (81.73%). In the case of Burg method, it is not easy to select the optimal order, due to this value varies for each subject. According to the obtained results the optimal order appears between 5 and 30, for higher orders the classification results are worse. The RMS parameter do not obtained always the best results, in some cases, the P_m performed better. However, the RMS seems to be the least affected with the order of AR model. The mean values present the RMS as the superior values, except for order 5.
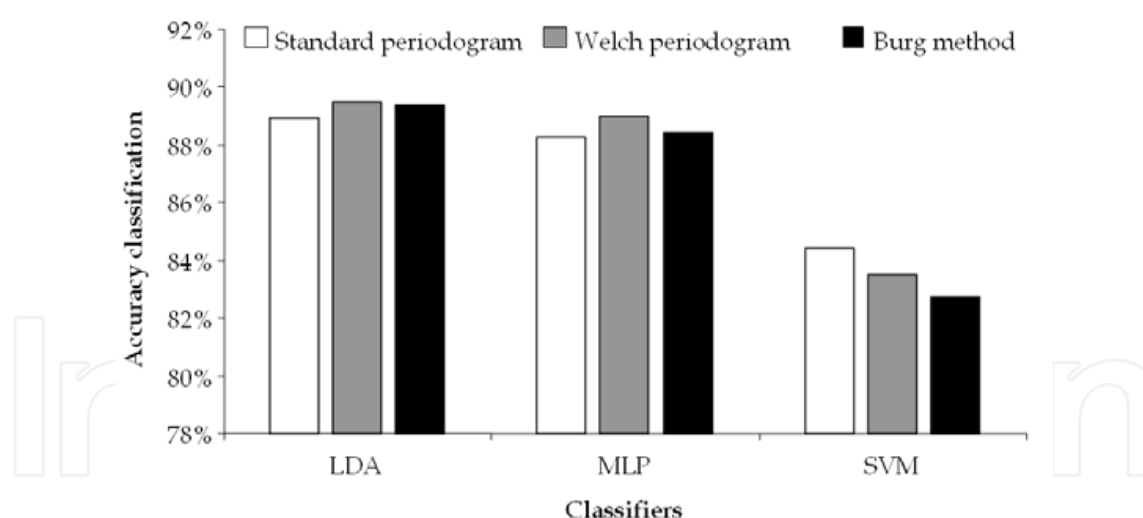

Fig. 14. Best accuracy classification obtained with each PSD estimation method proposed with the LDA, MLP and SVM.

In Figure 13, the advantages of use the Welch periodogram and the Burg method to estimate the PSD periodogram over the standard periodogram are shown. The standard periodogram obtain the worst results, except in S5 where Burg method performance is worse. Welch periodogram has better results in subjects S2 and S5 and the Burg method in the other subjects.

The mean value does not show big differences between these methods, i.e., standard periodogram, Welch periodogram and Burg method achieve 77.5%, 79.3% and 78% of accuracy classification over all subjects, respectively. In the same Figure, using the LVQ, similar results and conclusion are achieved; but with LVQ lower results are reached.

For the motor-imagery database, the RMS obtains better performances than P_m with the standard periodogram (see Figure 9) using any classifier. For Welch, the best results are reached with a window length of 64 and 32, i.e., a periodogram no so smoothed. Again the RMS presents higher values. In Burg method case, do not seem to be an optimal chose for AR model order. However, orders higher than 12 present a tendency to inferior results with any classifier and in the other side, the lower orders seems do not affect seriously the results. But with order lower than 6 it is expected that the periodogram do not describe accurately the EEG properties.

In Figure 14, the Welch periodogram present the best results using LDA and MLP. With SVM the best result is achieved by standard periodogram, but there is not a great difference between these values.

Although, out of the scope of this work, is presented a briefly comparison of the difference classifiers used in this work. The LDA present, almost in every case, good results, the MLP has a similar performance. The LVQ, do not obtain good results. The SVM obtain always lower values than LDA and MLP, but the difference is short. In the related bibliography, generally, the SVM achieve better results than other classification techniques. The poor results achieved in this work, are due possibly to the two nested cross-validation loops implemented in SVM training. This was made in order to obtain better future generalization performance and may be the results obtained with LDA and MLP are overvalued (Dornhege *et al.*, 2007).

8. Conclusions

In this work, parametric (Burg) and non parametric (standard and Welch) spectral methods were utilized in order to estimate the spectral content of EEG signals for different mental tasks. Two parameters were utilized to analyze the behaviour of every spectral estimation methods: the P_m and the RMS of different frequency bands. These methods were tested in two different databases.

We found that the use of the RMS allows higher classification accuracies with any spectral estimation technique. The Welch periodogram and Burg method are preferable in front of the standard periodogram. The use of Welch or Burg methods seems to be indistinct due to they performed similar, although in some subjects performed better one than other.

9. Acknowledgments

10. References

Akin, M. & Kiymik, M. K. (2000). Application of Periodogram and AR Spectral Analysis to EEG Signals. *Journal of Medical Systems,* Vol. 24, No. 4, (August, 2000), pp. 247-256, ISSN 0148-5598.

Bufalari, S.; Mattia, D.; Babiloni, F.; Mattiocco, M.; Marciani, M. G. & Cincotti, F. (2006). Autoregressive spectral analysis in Brain Computer Interface context, *Proceedings of the 28th IEEE EMBS Annual International Conference*, pp. 3736-3739, ISBN 1-4244-0032-5, New York, USA, Aug 30-Sept 3, 2006. IEEE press.

Chang, Chih-C. & Lin, Chih-J. (2008). LIBSVM: a Library for Support Vector Machines. Department of Computer Science National Taiwan University, Taiwan. Software available at http://www.csie.ntu.edu.tw/~cjlin/libsvm. Last updated: May 13, 2008

Diez, P. & Pi Marti, J. E. (2006). *Development of a classifier of electroencephalographic signals based on a microcontroller* (In Spanish) - Grade Thesis (May, 2006). pp. 22-57. Facultad de Ingeniería – Universidad Nacional de San Juan.

Dornhege, G.; Millán J. del R.; Hinterberger, T.; McFarland, D. J. & Müller, K-R. (2007) *Toward Brain-Computer Interfacing,* MIT Press. ISBN 978-0-262-04244-4. USA.

Ferreira, A.; Freire Bastos-Filho T. & Sarcinelli-Filho M.; Martín Sánchez, J.L.; García García J.C. & Mazo Quintas M. (2008) Evaluation of PSD components and AAR parameter as input features for a SVM classifier applied to a Robotic Wheelchair. *IBERDISCAP 2008*. Cartagena de Indias, Colombia. November 24-26, 2008.

Gil Flores, J.; García Giménez, E. & Rodríguez Gomez, G. (2001). *Books of Statistics Nº12: Discriminate Analysis* (in Spanish). Ed. La Muralla S.A. and Ed. Hespérides S.I. 2001. ISBN 84-7133-704-5. Spain.

Haykin, S. (1999). *Neural Networks A Comprehensive Foundation* , 2 Edition. 1999 - Ed. Pretince Hall. ISBN 0-13-273350-1. New Jersey, USA.

Hsu, Chih-W.; Chang, Chih-C. & Lin, Chih-J. (2008). A Practical Guide to Support Vector Classification. Department of Computer Science National Taiwan University, Taiwan http://www.csie.ntu.edu.tw/~cjlin/papers/guide/guide.pdf Last updated: May 21, 2008

Krusienski, D. J.; McFarland D. J. & Wolpaw J. R. (2006). An Evaluation of Autoregressive Spectral Estimation Model Order for Brain-Computer Interface Applications. *Proceedings of the 28th IEEE EMBS Annual International Conference*, pp.1323-1326, ISBN 1-4244-0032-5, New York USA, Aug 30-Sept 3, 2006. IEEE press.

Krusienski, D. J.; Schalk, G.; McFarland, D. J. & Wolpaw, J. R. (2007). A µ-Rhythm Matched Filter for Continuous Control of Brain-Computer Interface. *IEEE Trans. on Biomedical Engineering,* Vol.54, No.2, (Feb. 2007), pp. 273-280, ISSN 0018-9294.

Lotte, F.; Congedo, M.; Lécuyer, A.; Lamarche, F. & Arnaldi B. (2007). A review of classification algorithms for EEG-based brain-computer interfaces. *Journal of Neural Engineering,*Vol. 4, No.2, (January, 2007) pp. R1-R13, IOP Publishing, ISSN 1741-2560.

Kohonen, T. (1990). The Self-Organizing Map. *Procedings of IEEE*, Vol. 78, No. 9, (September, 1990) pp. 1464-1480, ISSN 0018-9219.

Mason, S. G. & Birch, G. E. (2003) A General Framework for Brain-Computer Interface Design. *IEEE Trans. on Neural systems and Rehabilitation Engineering,* Vol.11, No. 1, (March 2003), pp. 70-85, ISSN 1534-4320.

McFarland, D. J.; Anderson, C. W.; Müller, K.-R.; Schlögl, A. & Krusienski, D. J. (2006). BCI Meeting 2005—Workshop on BCI Signal Processing: Feature Extraction and Translation. *IEEE Trans. on Neural Systems and Rehabilitation Engineering*, Vol. 14, No. 2, (June 2006) pp. 135-138, ISSN 1534-4320.

Millán del R., J.; Mouriño, J.; Franzé, M.; Cincotti, F.; Varsta, M.; Heikkonen, J. & Babiloni, F. (2002). A Local Neural Classifier for the Recognition of EEG Patterns Associated to Mental Tasks. *IEEE Trans. on Neural Networks*, Vol.13, No. 3, (May 2002), pp. 678-686, ISSN 1045-9227.

Millán del R., J.; Renkens, F.; Mourino, J. & Gerstner, W. (2004) Brainactuated interaction. *Artif. Intel.*, vol. 159, no. 1–2 (Nov.2004), pp. 241–259. ISSN 0004-3702

Neuper, C.; Schlögl, A. & Pfurtscheller, G. (1999). Enhancement of left-right sensorimotor EEG differences during feedback-regulated motor imagery. *J. Clin Neurophysiol.* Vol. 16, No.4, (July ,1999), pp. 373-382, ISSN 0736-0258.

Palaniappan, R. (2006). Utilizing Gamma Band to Improve Mental Task Based Brain-Computer Interface Design. *IEEE Trans. on Neural Systems and Rehabilitation Engineering*, vol. 14, no. 3, (September, 2006), pp. 299-303, ISSN 1534-4320.

Pfurtscheller, G.; Lopes da Silva, F.H. (1999). Event-related EEG/MEG synchronization and desynchronization: basic principles. *Clinical Neurophysiology*, vol. 110, No.11, pp 1842-1857, ISSN 1388-2457.

Pfurtscheller, G.; Neuper, C.; Schlögl, A. & Lugger K. (1998). Separability of EEG signals recorded during right and left motor imagery using adaptive autoregressive parameters. *IEEE Trans Rehabil Eng.* Vol. 6, No. 3, (September, 1998), pp 316-325. ISSN 1063–6528.

Schlögl, A.; Lugger, K. & Pfurtscheller, G. (1997). Using Adaptive Autoregressive Parameters for a Brain-Computer-Interface Experiment, *Proceedings of the IEEE EMBS 19th Annual International Conference*, ISBN 0-7803-4262-3, pp.1533-1535, Chicago, IL, Oct 30-Sept 2, 1997, IEEE press.

Sörnmo, L. & Laguna, P. (2005) *Bioelectrical Signal Processing in Cardiac and Neurological Applications*, Elsevier Academic Press. ISBN 0-12-437552-9. USA.

Tinsley, H. E. A. & Brown, S. D. (2000). *Handbook of Applied Multivariate Statistics and Mathematical Modeling* 1st edition. Elsevier Academic Press, ISBN 0-12-691360-9.

Wolpaw, J. R.; Birbaumer, N.; McFarland, D. J.; Pfurtscheller, G. & Vaughan, T.M. (2002) Brain-computer interfaces for communication and control. *Clin. Neurophysiol.*, vol. 113, pp. 767–791, ISSN 1388-2457.

Biomedical Engineering

Edited by Carlos Alexandre Barros de Mello

ISBN 978-953-307-013-1

Hard cover, 658 pages

Publisher InTech

Published online 01, October, 2009

Published in print edition October, 2009

Biomedical Engineering can be seen as a mix of Medicine, Engineering and Science. In fact, this is a natural connection, as the most complicated engineering masterpiece is the human body. And it is exactly to help our "body machine" that Biomedical Engineering has its niche. This book brings the state-of-the-art of some of the most important current research related to Biomedical Engineering. I am very honored to be editing such a valuable book, which has contributions of a selected group of researchers describing the best of their work. Through its 36 chapters, the reader will have access to works related to ECG, image processing, sensors, artificial intelligence, and several other exciting fields.

How to reference

In order to correctly reference this scholarly work, feel free to copy and paste the following:

Pablo F. Diez, Eric Laciar, Vicente Mut, Enrique Avila and Abel Torres (2009). Classification of Mental Tasks using Different Spectral Estimation Methods, Biomedical Engineering, Carlos Alexandre Barros de Mello (Ed.), ISBN: 978-953-307-013-1, InTech, Available from: http://www.intechopen.com/books/biomedical-engineering/classification-of-mental-tasks-using-different-spectral-estimation-methods

INTECH
open science | open minds